THEORETICAL & APPLIED MECHANICS LETTERS **4**, 051002 (2014)

Effects of vacancy defect on the tensile behavior of graphene

Xiaoyu Sun,[a] Zuoguang Fu,[b] Mingtan Xia,[c] Yuanjie Xu[d]
Department of Engineering Mechanics, School of Civil Engineering, Wuhan University, Wuhan 430072, China

(Received 1 June 2014; accepted 31 July 2014)

Abstract Graphene is the strongest material but its performance is significantly weakened by vacancy defects. We use molecular dynamics simulations to investigate the tensile behavior of a graphene which contains a single vacancy defect. Our results suggest that because of the single vacancy, the fracture strength of graphene losses about 17.7%. The stress concentration around the vacancy defect leads to the destruction of nearby six-member rings structure, which forms the initial crack. The propagation direction of this crack in defective graphene is at an angle of 60° to the tensile direction initially, but then becomes perpendicular to the tensile direction.

© *2014 The Chinese Society of Theoretical and Applied Mechanics.* [doi:10.1063/2.1405102]

Keywords graphene, vacancy defect, fracture, molecular dynamics simulation

Graphene, exfoliation of a single atomic layer of graphite, is a hexagonal monolayer network of carbon atoms. The stiffness and fracture strength of this ultimate monolayer material are in the range of TPa and GPa, respectively.[1] The extraordinary mechanical properties make graphene a promising candidate in many kinds of fields,[2–6] e.g., surface coating, chemical sensors, and graphene-based nanocomposites.

There are numerous studies carried out on the strength and elastic properties of defect-free graphene via first-principle, molecular-dynamics, and continuum mechanics simulations. For instance, considering the C–C bonds network as a truss structure, Scarpa et al.[7] analytically described the effective mechanical properties of a monolayer graphene under in-plane tension. They gave theoretical expressions of Possion ratio and elastic moduli, which show slight difference with the results of finite element simulations. Volokh[8] analyzed how a single-atom-thick graphene sheet was destroyed in the plane tension under varying biaxiality condition by using a combined method of continuum and molecular mechanics. Similarly, Tuleubekov et al.[9] combined molecular and continuum mechanics by using Cauchy–Born rule to study the strength of a monolayer graphene which is under bi-axial tension. To determine the displacements of carbon atoms in a single-layer graphene after relaxation, Zhou and Huang[10] used molecular dynamics (MD) simulations to calculate the change of internal lattice of graphene under macroscopic strain. Wang and Zhang[11] calculated the Young's modulus and fracture stress of bilayer graphenes via MD simulations. It is found that for either zigzag or armchair graphene, both chirality and tensile loading direction have massive influence on their mechanical properties; for chiral bilayer graphenes, the

[a]Corresponding author. Email: xiaoyusun@whu.edu.cn.
[b]Email: zgfu1985@whu.edu.cn.
[c]Email: xiamingtan@whu.edu.cn.
[d]Corresponding author. Email: yj_xu@whu.edu.cn.

mechanical properties are not sensitive to the tensile loading direction.

In realistic graphene materials, some structural defects are always introduced as they are produced via mechanical exfoliation, chemical vapour deposition (CVD), or chemical reduction. It was found that mechanical properties of graphene are significantly influenced by defects. For example, Wang et al.[12] investigated the mechanical behaviors of defective graphene sheets which possess vacancies by using MD simulations and quantized fracture mechanics. They found that a remarkable loss of strength is caused by vacancies and the fracture strength is not only sensitive to the loading directions but also to the temperature. Carpenter et al.[13,14] reported the vacancy-induced amorphization and the mechanical properties of irradiated single-layer graphene via MD simulations. The vacancy defect was generated by a vacancy insertion simulation model, and they determined a critical range of vacancy concentrations which leads to a qualitative change in the fracture response from brittle to ductile. By coupling the quantum calculations and molecular simulations, Khare et al.[15] studied the fracture behavior and cracks expansion of defective graphenes, and showed that Griffith formula can well describe the fracture stresses when the defect is smaller than 1 nm. Zhao and Aluru[16] used MD simulations to investigate the relationship between the reduced fracture strength of a monolayer graphene and temperature, loading rate, and characteristic length of cracks. The MD simulation results are compared with the deduction of quantized fracture mechanics theory, showing that large inclusion holes will strongly reduce the graphene strength while vacancy only slightly decreases the Young's modulus.

Despite of the recent progress, little is known about the evolution of defective graphene morphology during tension. In the present work, we use MD simulations to study how a single vacancy influences the tensile strength of a single layer graphene sheet. Moreover, the morphology evolution of the graphene with a single vacancy in its centre is also investigated.

Our structural model used in simulations is depicted in Fig. 1. Both the length and width of the graphene are set as 20 nm. In the adopted cartesian coordinate system, the x-axis and y-axis are set along the zigzag and the armchair directions, respectively, and the z-axis is normal to the graphene. Periodic boundary conditions are adopted in all the three directions. Figure 1(b) shows an enlarged view of the vacancy defect in Fig. 1(a). The vacancy defect is introduced by deleting a carbon atom in the center of graphene. Our MD simulations are performed using the LAMMPS.[17] The adaptive interatomic reactive empirical bond-order (AIREBO) potential[18] is adopted to depict the interlayer interactions of carbon atoms in the graphene, which has been shown to be quite advantageous for understanding the phenomena in carbon systems.[19,20]

Prior to loading, we use conjugate gradient method to relax the defective graphene to the configuration which possesses minimum energy. Then, a Nosé–Hoover thermostat is employed to thermally equilibrated the system for 50 ps. The time step is chosen as 1 fs. Simulations are run at temperatures of 1 K and 300 K, respectively. To avoid thermal disturbance in the case of 300 K, we show the simulation results at 1 K in this work. After relaxation, uniaxial tension is applied by stretching the cubic box along the x-direction. The strain rate of loading is set as 10^9 s^{-1}. This stepwise straining method is commonly used in MD simulations of various materials.[21–23] In our simulation, we calculate the atomic-lever stresses by using Virial theorem.[24]

The tensile stress–strain curve for the defective graphene is shown in Fig. 2. For comparison, the stress of a defect-free graphene is also given. At the initial deformation stage (up to

about 0.05), the stress increases linearly with strain. The elastic modulus is commonly defined as the corresponding slope.[25] When the strain is at higher level, the stress–strain curve shows a nonlinear tendency. The stress continues to increase, until it reaches a maximum value, which is assumed as the ultimate strength. The fracture strength of the defect-free and defective graphene is 116.2 GPa and 95.7 GPa, and the rupture strain is 0.284 and 0.156, respectively. It is seen that due to the single vacancy, the fracture strength of graphene have a loss of about 17.7%. Wang et al.[12] have studied the effect of vacancy on fracture strength of graphene by considering the defect in graphene as a crack. For a graphene with n vacancies, the fracture strength σ_f can be deduced as $\sigma_f(n) = \sigma_c\sqrt{1+\rho/(2\sqrt{3}a)}\,(1+n)^{-0.5}$, where σ_c is the strength of defect-free graphene, a is bond length of C–C and ρ is the crack tip radius. In this case, $n = 1$ and $\rho = 0.8l_0$, $l_0 = \sqrt{3}a$ is the lattice spacing, so the fracture strength is $0.836\sigma_c$, which matches our simulation results very well.

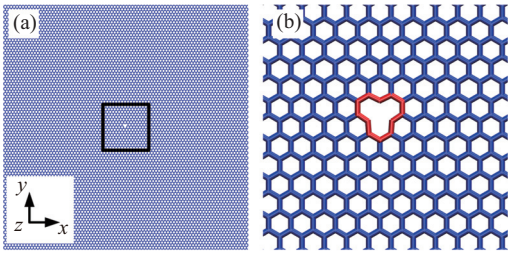

Fig. 1. Simulation model. (a) A single vacancy defect is in the center of a graphene layer. (b) Enlarged view of the vacancy defect.

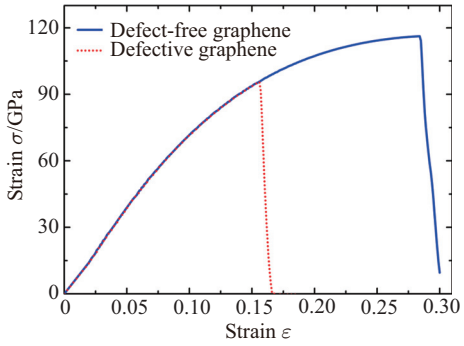

Fig. 2. Tensile stress–strain curve for the defect-free and defective graphenes.

To further reveal how the defective graphene ruptures, we explore the evolution of microstructure. Figure 3 presents a sequence of snapshots, and the carbon atoms are in colored according to their atomic stress. Figure 3(a) shows the atomic configuration and atomic stress distribution of the defective graphene at the strain of $\varepsilon = 0.154$. It is observed that stress concentration occurs around the vacancy. The atoms which have the maximum stress are located in the y direction while the minimum stress atoms are located in the x direction of defect. The maximum and minimum stress are 149 GPa and 21.5 GPa, respectivly. As shown in Fig. 3(a), two C–C bonds a_1 and a_2 around the vacancy defect are most likely to break. As the applied strain exceeds a critical value of $\varepsilon = 0.155$, one of these two most dangerous bonds is broken stochastically (a_2 in Fig. 3(b)), leading to the destruction of the structure of six-member rings (circle in Fig. 3(b)). As the strain further increases from $\varepsilon = 0.155$ to $\varepsilon = 0.156$, C–C bonds in a series of rings exhibit successive rupture (circle in Fig. 3(c)). The newly broken C–C bonds are parallel to the firstly broken C–C bond a_2, which is easier to release energy. Therefore, the angle between the direction of crack propagation (arrow in Fig. 3(c)) and the x axis is 60°. The crack continues to propagate after strain reaches $\varepsilon = 0.156$. However, the direction becomes perpendicular to the tensile direction (Fig. 3(d)) at strain $\varepsilon = 0.157$. Then, the crack propagates in this direction (arrows in Fig. 4) until complete rupture.

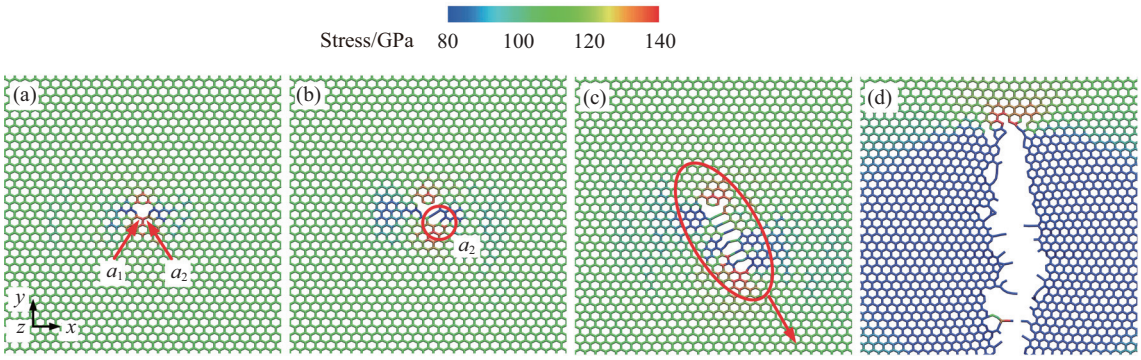

Fig. 3. Atomic configuration and atomic stress distribution evolution of the defective graphene at the strain of (a) $\varepsilon = 0.154$, (b) $\varepsilon = 0.155$, (c) $\varepsilon = 0.156$, and (d) $\varepsilon = 0.157$. Carbon atoms are colored according to their atomic stress.

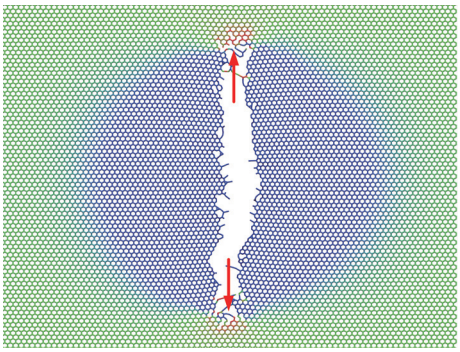

Fig. 4. Configuration of the defective graphene at the strain of $\varepsilon = 0.158$.

In summary, the tensile deformation behaviors of defective graphene have been investigated using MD simulations. It is found that the fracture strength of graphene losses about 17.7% due to the single vacancy. The vacancy defect in the graphene centre induces stress concentration, which further leads to the destroy of six-member rings structure around the vacancy. The propagation direction of crack in defective graphene is at an angle of 60° to the tensile direction initially, but then becomes perpendicular to the tensile direction. Our results may provide atomic-scale information for understanding the mechanical behaviors of defective graphenes.

This work was supported by the Open Research Fund Program (2042014kf0002) of Wuhan University, the National Natural Science Foundation of China (11372230), and the Open Research Fund Program (HBKLWJ-2014F02) of Key Laboratory of Hubei Province for Water Jet Theory & Technology.

1. C. Lee, X. Wei, J. W. Kysar, et al. Measurement of the elastic properties and intrinsic strength of monolayer graphene. *Science* **321**, 385–388 (2008).
2. F. Schedin, A. K. Geim, S. V. Morozov, et al. Detection of individual gas molecules adsorbed on graphene. *Nature Materials* **6**, 652–655 (2007).
3. X. Li, X. Wang, L. Zhang, et al. Chemically derived, ultrasmooth graphene nanoribbon semiconductors. *Science* **319**, 1229–1232 (2008).
4. S. Stankovich, D. A. Dmitriy, G. H. B. Geoffrey, et al. Graphene-based composite materials. *Nature* **442**, 282–286 (2006).
5. M. A. Rafiee, W. Lu, A. V. Thomas, et al. Graphene nanoribbon composites. *ACS Nano* **4**, 7415–7420 (2010).

6. M. A. Rafiee, J. Rafiee, Z. Wang, et al. Enhanced mechanical properties of nanocomposites at low graphene content. *ACS Nano* **3**, 3884–3890 (2009).
7. F. Scarpa, S. Adhikari, P. A. Srikantha. Effective elastic mechanical properties of single layer graphene sheets. *Nanotechnology* **20**, 065709 (2009).
8. K. Y. Volokh. On the strength of graphene. *Journal of Applied Mechanics* **79**, 064501 (2012).
9. K. Tuleubekov, K. Y. Volokh, H. Stolarski, et al. Strength of graphene in biaxial tension. *European Journal Mechanics A/Solids* **39**, 291–297 (2013).
10. J. Zhou, R. Huang. Internal lattice relaxation of single-layer graphene under in-plane deformation. *Journal of Mechanics and Physics of Solids* **56**, 1609–1623 (2008).
11. L. Wang, Q. Zhang. Elastic behavior of bilayer graphene under in-plane loadings. *Current Applied Physics* **12**, 1173–1177 (2012).
12. M. C. Wang, C. Yan, L. Ma, et al. Effect of defects on fracture strength of graphene sheets. *Computational Materials Science* **54**, 236–239 (2012).
13. C. Carpenter, A. Ramasubramaniam, D. Maroudas. Analysis of vacancy-induced amorphization of single-layer graphene. *Applied Physics Letters* **100**, 203105 (2012).
14. C. Carpenter, D. Maroudas, A. Ramasubramaniam. Mechanical properties of irradiated single-layer graphene. *Applied Physics Letters* **103**, 013102 (2013).
15. R. Khare, S. L. Mielke, J. T. Paci, et al. Coupled quantum mechanical/molecular mechanical modeling of the fracture of defective carbon nanotubes and graphene sheets. *Physical Review B* **75**, 075412 (2007).
16. H. Zhao, N. R. Aluru. Temperature and strain-rate dependent fracture strength of graphene. *Journal of Applied Physics* **108**, 064321 (2010).
17. S. Plimpton. Fast parallel algorithms for short-range molecular dynamics. *Journal of Computational Physics* **117**, 1–19 (1995).
18. S. J. Stuart, A. B. Tutein, J. A. Harrison. A reactive potential for hydrocarbons with intermolecular interactions. *Journal of Chemical Physics* **112**, 6472–6486 (2000).
19. Y. Dong, Y. He, Y. Wang, et al. A theoretical study of ripple propagation in defective graphene. *Carbon* **68**, 742–747 (2014).
20. Y. I. Jhon, Y. Min, G. Y. Yeom. Orientation dependence of the fracture behavior of graphene. *Carbon* **66**, 619–628 (2013).
21. A. C. To, J. Tao, M. Kirca, et al. Ligament and joint sizes govern softening in nanoporous aluminum. *Applied Physics Letters* **98**, 051903 (2011).
22. J. Schiøtz, K. W. Jacobsen. A maximum in the strength of nanocrystalline copper. *Science* **301**, 1357–1359 (2003).
23. W. W. Liang, M. Zhou. Shape memory effect in Cu nanowires. *Nano Letters* **5**, 2039–2043 (2005).
24. A. J. Cao,Y. G. Wei. Atomistic simulations of the mechanical behavior of fivefold twinned nanowires. *Physical Review B* **74**, 214108 (2006).
25. B. Mortazavi, Y. Rémond, S. Ahzi, et al. Thickness and chirality effects on tensile behavior of few-layer graphene by molecular dynamics simulations. *Computational Materials Science* **53**, 298–302 (2012).